Micro-, Meso-, and Macroporous Carbons Supported Pt catalysts and Their Electrocatalytic Performances during Methanol Oxidation Reaction

An-Ya Lo (駱安亞)[1,2], Chin-Te Hung (洪錦德)[1], Shou-Heng Liu (劉守恆)[3], Cheng-Tzu Kuo (郭正次)[4], and Shang-Bin Liu (劉尚斌)[1,5,*]

[1] Institute of Atomic and Molecular Sciences, Academic Sinica, Taipei 10617, Taiwan

[2] Green Energy Development Center, Fong Chia University, Taichung 40724, Taiwan

[3] Department of Chemical and Materials Engineering, National Kaohsiung University of Applied Sciences, Kaohsiung 80778, Taiwan

[4] Department of Materials Science and Engineering, National Chiao Tung University, Hsingchu 30010, Taiwan

[5] Department of Chemistry, National Taiwan Normal University, Taipei 11677, Taiwan

*E-Mails: sbliu@sinica.edu.tw

Abstract

Carbon porous materials (CPMs) with pore size ranging from 2 to 50 nm have been widely studied as catalyst support materials in direct methanol fuel cells (DMFCs). However, the potential of microporous (< 2 nm) and macroporous (> 50 nm) carbons have been largely overlooked. Herein, a novel nanofabrication process was developed to replicate micro-, meso-, and macroporous carbons from various porous silica templates, such as zeolites, mesoporous silicas (MCM-41, MCM-48, and SBA-15), and photonic crystals. These CPMs were then incorporated with Pt catalyst by impregnation method followed by reducing the platinum acetylacetonate. The resultant Pt/CPMs were characterized by TEM, Raman and XPS spectroscopy, N_2 adsorption/desorption isotherm, cyclic voltammetry (CV), competitive (CO vs. H_2) chemisorption, and electrical conductivity analyses. Regarding to the electrocatalytic performances of these Pt/CPMs during methanol oxidation reaction (MOR) in DMFC at anode, the peak forward mass activity I_f (from 122 to 655 A/g of Pt) in the CV curves, which is an index representing the MOR activity, was found to increase with increasing pore size of CPMs. On the other hand, in view of the CO-tolerance at anode, as inferred by the peak forward vs. reverse mass activity ratio of the CV curves (i.e., I_f/I_r), supported anodic catalysts abundant with smaller Pt particles (especially those with sizes < 1nm) are preferred.

Keywords: Carbon porous materials, CVI prosess, DMFC, Pt-based electrocatalyst, methanol oxidation reaction.

1. Introduction

In view of the increasing demands in environmental issues, DMFCs have becoming promising portable power sources. In which, the anodic electrodecatalysts commonly used nowadays are mostly noble metal (Pt or Pt-based) alloys supported on carbon materials. As such, metal catalyst dispersed carbon materials are critical to the overall performances of fuel cell electrodes [1,2]. Therefore, R&D of CPMs [3-5], carbon nanotubes (CNTs) [6], and activated carbons [7] possessing high surface areas, electrical conductivities, and electrochemical stabilities have drawn considerable attentions over the past years.

Regarding to the performance of DMFC, the methanol oxidation reaction (MOR) activity and CO tolerance are key issues on anodic catalyst. A well dispersed Pt catalyst dominates the anodic MOR activity. Whereas PtRu alloy catalyst performs a better CO tolerance on anodic electrodecatalysts [3-5,8,9]. However, PtRu catalysts are cost ineffectiveness. Therefore, Pt catalyst incorporated with various transition metals, such as Fe, Co, Ni, and Mo, have been extensively studied as CO-tolerance catalysts [10,11]. Other than that, carbon mesoporous materials can also provide some tolerance on CO poisoning [3], which mechanism is not

well-understood and may have great improvement in the further development on DMFC anode.

As for the application of carbon porous materials (CPMs) on DMFC, the investigations were mostly focused on CMMs with pore size ranging from 2 to 50 nm, while overlooking the potential applications of microporous (< 2 nm) and macroporous (> 50 nm) carbons. In order to understand the effect of pore size of CPMs on the performance of DMFC at anode, a series of CPMs with pore size ranging from micro-, meso-, to macroporous carbons, such as the ZRC, CMT-1, CMT-2, HCC, and PCC materials respectively prepared by using zeolite-Y, MCM-48, SBA-15, melted MCM-48, and photonic crystal as templates, have been fabricated by CVI process [12]. These materials were applied as the catalyst supports for DMFC anode and their MOR activity and CO-tolerance were evaluated and compared.

2 Experimental

2.1. Preparation of carbon porous materials

For the preparation of carbon porous materials, porous silica including MCM-48, SBA-15, and photonic crystal were urged as templates [13-15]. CPMs synthesized using various templates were conducted by similar procedures summarized below: first, the template was placed into a quartz reactor, followed by heating the reactor to the target temperature (1073 or 1093 K) under vacuum. Then, a desirable flow of acetylene was introduced into the reactor together with mixture of H2 and/or Ar gases. Then, the CPMs products may be respectively collected by filtering and drying after removal of silica template by etching with 1 M HF solution of 50% ethonal–50% H2O. Detailed preparation conditions for various CPMs are depicted in **錯誤! 找不到參照來源。**.

2.2. Preparation of carbon nanostructure supported DMFC electrocatalysts

To further explore their applications in fuel cell, the aforementioned CPMs were utilized as support for noble metal (Pt) catalyst. A hydrogen reduction process was adopted to disperse Pt on various carbon supports, typically, by first suspending ca. 0.2 g of the carbon in H_2PtCl_6 aqueous solution (10 mL H_2PtCl_6, 0.04 M) at room temperature, followed by drying in a vacuum evaporator and reduction treatment at 523 K for 30 min under H_2 atmosphere. The electrocatalysts are denoted as Pt/XC-72, Pt/ZRC, Pt/CMT-1, Pt/CMT-2, Pt/HCC, and Pt/PCC, respectively.

Table 1. Sample designations, processing conditions and diameters of CPMs and CNTs prepared by thermal TA-CVI without gas preheating.

Sample[a]	t (min)[b]	Template[c]	Gas flow ($C_2H_2/H_2/Ar$)[d]	T_S (K)[e]	d (nm)[f]
ZRC	40	Zeolite-Y	50/50/50	1073	< 1.3
CMT-1	40	MCM-48	50/50/50	1073	~ 2
CMT-2	60	SBA-15	50/50/0	1073	~ 3
HCC	40	MCM-48	50/50/0	1093	20 ~150
PCC	120	PC	50/50/0	1073	~ 400

a Prepared in the absence of a catalyst and without gas preheating; pressure = 3 kPa.
b Duration of processing time.
c Porous silica template used for producing CPMs.
d In unit of sccm:sccm:sccm.
e Substrate temperature during CVI process.
f Pore diameter of porous carbon.

2.3. Characterization

The microstructure of specimens were examined by TEM analysis (JEOL JEM-2100; 200 keV). The structuring ordering of the porous materials were examined by X-ray diffraction (XRD) patterns by using a PANalytical (X'Pert PRO) instrument using Cu Kα radiation (λ = 0.1541 nm). Thermogravimetric analyses (TGA) were performed using a Netzsch TG-209 instrument under dried air atmosphere. The BET surface areas and pore size distributions of various porous materials, were evaluated by nitrogen adsorption/desorption measurements conducted at 77 K using a Quantachrome Autosorb-1 analyzer after each sample was degassed at 200 ℃ under vacuum for at least 12 h. The electrodechemical properties of various supported carbon substrates as electrode materials were evluated by cyclic voltammetry (CV) measurements conducted on a galvanostat/potentiostat (Autolab, PGSTAT30). The dispersions and the CO tolerance of Pt/CPMs were measured by hydrogen chemisorption and competitive adsorption on an automated chemisorption apparatus (Micromeritics, AutoChem II 2920).

3 Results and discussion

3.1. Effect of carbon pore size on Pt dispersion in DMFC anodes and their electrocatalytic performance

A diversified carbon materials with micro- (ZRC), Meso- (CMT-1, CMT-2, HCC), and macroporous (PCC) may be fabricated using zeolites, MCM-48, SBA-15, and

photonic crystal as templates (錯誤! 找不到參照來源。).

The CPMs listed in Table 1 with varied pore characteristics (Table 2) were further applied as supports for Pt, the physical and electrochemical properties of the Pt/CPM supported catalyst were examined and compared with that of a commercial catalyst, namely Pt/XC-72, as depicted in Tab. 3. Note that since According to the ratio of the G- and D-band intensities (I_G/I_D) obtained from the Raman spectrum, similar I_G/I_D ratios were observed for the CPMs and XC-72 indicates that these types of carbon materials have roughly the same degree of graphization and hence electronic properties (Table 3).

The TEM images of various Pt/CPMs are shown in Fig. 1. Among them, the Pt/ZRC sample appears to have the highest Pt dispersion, as shown in Fig. 1a. The above observation may be attributed to the fact that, unlike other CPMs, the ZRC carbon support possesses only microporosities. As such, it is hypothesized that the porosity of the carbon support may play an important role while incorporating the Pt metal catalyst. By comparison, the percentage of the small (size < 1 nm) Pt nanoparticle presented in various carbon supports appear to follow the trend: Pt/ZRC (38%) > Pt/CMT-2 (30%) ~ Pt/CMT-1 (27%) > Pt/HCC (15%) > Pt/PCC (8%) ~ Pt/XC-72 (6%). Consequently, the former shows a high metallic surface area and superior electrocatalytic performances (Table 3) in terms of I_f/I_r ratio and resistance to CO poisoning, i.e. *CO-t* value.

Table 2. Comparison of specific surface areas for various CPM samples.

Sample	Specific surface area (m^2/g)[a]		
	Micropores	Mesopores	Macropores
ZRC	1235	647[b]	N/A
CMT-1	← 1229[c] →		N/A
CMT-2	N/A	1194	N/A
HCC	N/A	← 783[d] →	
PCC	N/A	N/A	337
XC-72	N/A	N/A	218

[a] N/A: surface area in these ranged are either negligible or unaccountable by the BJH method.
[b] Value estimated by subtracting the microporous surface area (determined by t-plot analysis) from the total BET surface area.
[c] CMT-1 possesses two types of pore systems, which span over the micro- and mesoporous ranges.
[d] Since its BET surface area may not be derived in this pore range, total surface area of the substrate was adopted.

Furthermore, the electrocatalystic performances of Pt/XC-72 and various Pt/CPMs supported catalysts during methanol oxidation reaction (MOR) were examined by cyclic voltammograms (CV) measurements under 1.0 M CH_3OH and 0.5 M H_2SO_4 at room temperature. For convenience, electrocatalytic properties of various Pt/CPMs, including their electronic conductivities (C), current densities (I_f & I_r), I_f/I_r and I_G/I_D ratios, tolerneces for CO poisoning (CO-t), and the dispersions (*D*), particle sizes (D_p), and metallic surface areas (S_M) of the Pt metal particles are depicted in Table 3 together with the Pt/XC-72 commercial catalyst.

Table 3. Assorted physicochemical properties of various Pt/CPMs and Pt/XC-72 electrocatalysts.

Sample	Pt[a] wt %	C[b] S/cm	I_G/I_D[c]	I_f[d] (mA)	I_r[d] (mA)	I_f/I_r[d]	D[e] (%)	D_p[f] (nm)	S_M[g] $m^2\ gPt^{-1}$	CO-t[h] (%)
Pt/ZRC	12.5	1.61	0.85	122	25	4.88	45.4	2.49	112.1	48.83
Pt/CMT1	12.8	1.14	0.68	136	60	2.26	22.4	5.05	55.4	27.93
Pt/CMT2	11.6	1.1	0.77	140	97	1.44	19.8	5.71	48.9	18.14
Pt/HCC	9.3	2.07	0.74	282	194	1.45	20.5	5.51	50.7	10.60
Pt/PCC	9.5	2.38	0.73	655	628	1.04	56.8	1.99	140.42	7.78
Pt/XC72	12.5	1.79	0.70	353	349	1.01	32.6	3.47	80.6	1.74

[a] Pt loading determined by TGA analysis.
[b] Electrical conductivity.
[c] Relative peak intensities obtained from the G- and D-bands of the Raman spectrum.
[d] Ratio of maximum current densities obtained from the forward (I_f) and reverse (I_r) scans of the CV curves.
[e] Pt dispersion measured by H_2 chemisorption (at 305 K).
[f] Pt particle size derived from H_2 chemisorption results.
[g] Metallic surface area of the Pt nanoparticles derived from H_2 chemisorption.
[h] CO-tolerance estimated by competitive adsorption of H_2 after pre-adsorbing ca. 500 ppm of CO.

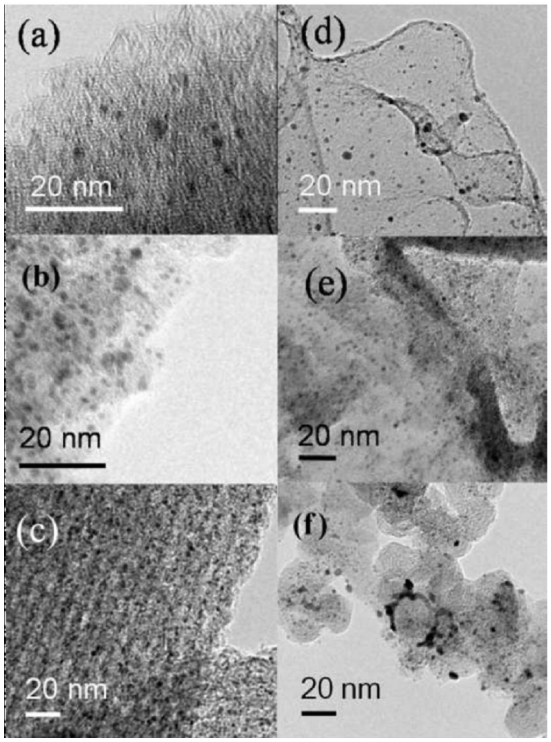

Fig. 1. TEM images of (a) Pt/ZRC, (b) Pt/CMT-1, (c) Pt/CMT-2, (d) Pt/HCC, (e) Pt/PCC, and (f) Pt/XC-72 electrocatalysts.

Since Pt/ZRC is more aboundant with small Pt nanoparticles (size < 1 nm), the sample is anticipated to have a superior electrocatalytic performance as anodic catalyst than the other Pt/CPMs. However, Pt/ZRC appeared to have a lower forward peak current (I_f) than the others (Fig. 2 and Table 3). It is noted that the degree of graphization (i.e., the I_G/I_D value) and conductivities (C) appeared to be irreverent to the value of I_f, rather, the latter tends to increase with increasing pore size of the carbon supports. For example, an I_f value of ca. 160 mA/mg Pt was observed for the Pt/ZRC, Pt/CMT-1, and Pt/CMT-2 catalysts; which are only one-half of what observed for the Pt/XC-72 catalyst (I_f ca. 353 mA/mg Pt). The above result may be attributed to the possibility that the Pt nanoparticles immerged in the porous CPMs may not be fully exposed to the methanol solution during C-V measurements. In other words, diffusion of methanol may be partially hindered in the micropores/mesopores of the CPMs during the CV tests, implying that internal surface areas within microporous/mesoporous CPM supports have nearly no effect on the overall electrocatalytic performances of the Pt/CPM electrocatalysts.

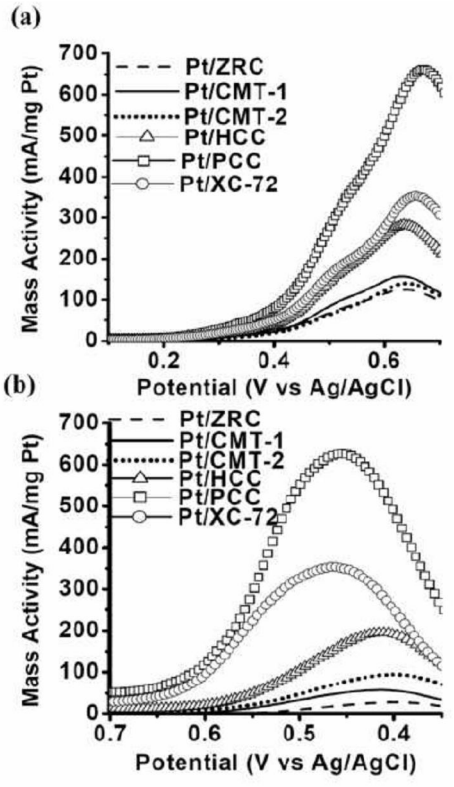

Fig. 2. (a) Forward and (b) reverse CV scans of various Pt/CPMs and Pt/XC-72 electrocatalysts.

On the other hand, the Pt/PCC catalyst appeared to have the largest forward anodic peak current (I_f) among various Pt/CPMs, even though its carbon support (PCC) possesses only ca. one-third of the surface area compared to CMT-1 and CMT-2. The aforementioned results may be associated with the fact that the surface area observed was predominantly from the external surfaces of the PCC. Similar observation was observed for the Pt/HCC catalyst. The same argument prevails for the observed increase in I_f value by ca. 1.8 folds in the Pt/PCC than the Pt/XC-72.

Considering the effect of pore size on catalytic performances of the Pt/CPM catalysts, the relative ratio of I_f/I_r may be served as an index to evaluate the tolerance for CO poisoning (*CO-t*), as listed in Table 3. It is intriguing that even though the Pt/ZRC catalyst exhibited a lower forward peak current (I_f) than the other Pt/CPMs, a superior value of I_f/I_r ratio was observed compared to Pt/XC-72 and other Pt/CPMs. Moreover, the I_f/I_r ratio observed for Pt/CPMs is found to increases with decreasing pore size of CPMs (Table 3) and with increasing percentage of small Pt nanoparticle with size < 1 nm.

To further justify the above findings, additional pulsed H2 chemisorption studies were conducted in the presence of the pre-adsorbed CO (ca. 500 ppm), which represents a competitive adsorption of CO with H_2. Accordingly, the corresponding dispersions (D), particle sizes (D_p), and metallic surface areas (S_M) of the Pt metal are depicted in Table 3. For examples, a S_M value of ca. 112 m2/g Pt was observed for the Pt/ZRC sample, among them, ca. 47% of the metal surfaces remain active after the catalyst was intentionally poisoned by pre-adsorbing 500 ppm of CO. Whereas in the case of Pt/XC-72, nearly all metal Pt surfaces were inactivated by pre-adsorbed CO. The same trend for activity may be inferred by comparing the I_f/I_r and *CO-t* values of Pt/CPMs vs. Pt/XC-72 supported catalysts.

4. Conclusion

In brief, various carbon porous materials (CPMs), namely ZRC, CMT-1, CMT-2, HCC, and PCC, were successfully synthesized by the improved thermal CVI process developed herein using different micro-, meso- and macro-porous siliceous materials such as zeolites, mesoporous silicas, and photonic crystal as templates. The

pore dimensions of these CPMs were found to follow the order: ZRC < CMT-1 < CMT-2 < HCC < PCC. It was found that carbon supports with smaller pore dimensions are more favorable in terms of dispersing Pt nanoparticles typically in the order of a few nm. Nevertheless, in the case of using Pt/ZRC as supported electrodecatalyst during methanol oxidation reaction, even though that majority of the incorporated Pt metal particles are less than 1 nm in size, restricted diffusion of methanol hindered by the microporous ZRC carbon resulted in poor catalytic performance. On the other hand, macroporous PCC, which possesses a large external surface area, exhibits superior catalytic performance during methanol oxidation. Thus, it is conclusive that CPM supports with smaller pore sizes are more favorable for dispersion of Pt nanoparticiles, particularly for paticles with size less than 1 nm, leading to an increase in CO tolerance in various Pt/CPMs catalyhst. In this context, future works aiming at preparation of CPMs supported catalyst with metal particle size less than ca. 1 nm should be an interesting and demanding task.

Acknowledgments The supports of this work by the the National Science Council, Taiwan (NSC98-2113-M-001-017-MY3 and NSC101- 2218-E-035-005) are gratefully acknowledged.

References

[1] J. Qi, L. Jiang, Q. Tang, S. Zhu, S. Wang, B. Yi, G. Sun. "Synthesis of graphitic mesoporous carbons with different surface areas and their use in direct methanol fuel cells." *Carbon*, **50**, 2824, 2012.

[2] D. J. You, K. Kwon, S. H. Joo, J. H. Kim, J. M. Kim, C. Pak, H. Chang. "Carbon-supported ultra-high loading Pt nanoparticle catalyst by controlled overgrowth of Pt: Improvement of Pt utilization leads to enhanced direct methanol fuel cell performance" *Inter. J. Hydro. Energy*, **37**, 6880, 2012.

[3] S. H. Liu, R. F. Lu, S. J. Huang, A. Y. Lo, S. H. Chien, S. B. Liu. "Controlled synthesis of highly dispersed platinum nanoparticles in ordered mesoporous carbons." *Chem Commun*., **32**, 3435, 2006.

[4] S. H. Liu, W. Y. Yu, C. H. Chen, A. Y. Lo, B. J. Hwang, S. H. Chien, S. B. Liu. "Fabrication and characterization of well-dispersed and highly stable PtRu nanoparticles on carbon mesoporous material for applications in direct methanol fuel cell." *Chem. Mater.*, **20**, 1622, 2008.

[5] T. Maiyalagan, T. O. Alaje, K. Scott. "Highly Stable Pt–Ru Nanoparticles Supported on Three-Dimensional Cubic Ordered Mesoporous Carbon (Pt–Ru/CMK-8) as Promising Electrocatalysts for Methanol Oxidation." *J. Phys. Chem. C*, **116**, 2630, 2011.

[6] A. Y. Lo, N. Yu, S. J. Huang, C. T. Hung, S. H. Liu, Z. Lei, C. T. Kuo, S. B. Liu. "Fabrication of CNTs with controlled diameters and their applications as electrocatalyst supports for DMFC." *Diamond Related Mater.*, **20** 343, 2011.

[7] G. G. Park, T. H. Yang, Y. G. Yoon, W. Y. Lee, C. S. Kim. "Pore size effect of the DMFC catalyst supported on porous materials." *Inter. J. Hydro. Energy*, **28**, 645, 2003.

[8] X. M. Ren, P. Zelenay, S. Thomas, J. Davey, S. Gottesfeld. "Recent advances in direct methanol fuel cells at Los Alamos National Laboratory." *J. Power Sources*, **86**, 111, 2000.

[9] M. L. Lin, M. Y. Lo, C. Y. Mou. "PtRu nanoparticles supported on mesoporous carbon thin film as highly active anode materials for direct methanol fuel cell." *Catal. Today*, **160**, 109, 2011.

[10] J. Xu, K. Hua, G. Sun, C. Wang, X. Lv, Y. Wang. "Electrooxidation of methanol on carbon nanotubes supported Pt–Fe alloy electrode." *Electrochem. Commun.*, **8**, 982, 2006.

[11] H. Zhao, J. Dong, S. Xing, Y. Li, J. Shen, J. Xu. "Electrochemical oxidation of small organic molecules on hydrothermal synthesized Pt and PtCo/ordered mesoporous carbon." *Inter. J. Hydro. Energy*, **36**, 9551, 2011.

[12] A. Y. Lo, S. J. Huang, W. H. Chen, Y. R. Peng, C. T. Kuo, S. B. Liu. "Template-assisted synthesis of mesoporous tubular carbon nanostructure by chemical vapor infiltration method." *Thin Solid Films*, **498**, 193, 2006.

[13] J. M. Kim, S. K. Kim, R. Ryoo. "Synthesis of MCM-48 single crystals." *Chem. Commun.*, **2**, 259, 1998.

[14] D. Zhao, J. Feng, Q. Huo, N. Melosh, G. H. Fredrickson, B. F. Chmelka, G. D. Stucky. "Triblock copolymer syntheses of mesoporous silica with periodic 50 to 300 angstrom pores." *Science*, **279**, 548, 1998.

[15] B. T. Holland, C. F. Blanford, T. Do, A. Stein. "Synthesis of highly ordered, three-dimensional, macroporous structures of amorphous or crystalline inorganic oxides, phosphates, and hybrid composites." *Chem. Mater.*, **11**, 795, 1999.